Efficient targeted mutagenesis in the monarch butterfly using zinc-finger nucleases

Christine Merlin,[1,5] Lauren E. Beaver,[1] Orley R. Taylor,[2] Scot A. Wolfe,[3,4] and Steven M. Reppert[1,5]

[1]*Department of Neurobiology, University of Massachusetts Medical School, Worcester, Massachusetts 01605, USA;* [2]*Department of Ecology and Evolutionary Biology, University of Kansas, Lawrence, Kansas 66045, USA;* [3]*Program in Gene Function and Expression, University of Massachusetts Medical School, Worcester, Massachusetts 01605, USA;* [4]*Department of Biochemistry and Molecular Pharmacology, University of Massachusetts Medical School, Worcester, Massachusetts 01605, USA*

The development of reverse-genetic tools in "nonmodel" insect species with distinct biology is critical to establish them as viable model systems. The eastern North American monarch butterfly (*Danaus plexippus*), whose genome is sequenced, has emerged as a model to study animal clocks, navigational mechanisms, and the genetic basis of long-distance migration. Here, we developed a highly efficient gene-targeting approach in the monarch using zinc-finger nucleases (ZFNs), engineered nucleases that generate mutations at targeted genomic sequences. We focused our ZFN approach on targeting the type 2 vertebrate-like *cryptochrome* gene of the monarch (designated *cry2*), which encodes a putative transcriptional repressor of the monarch circadian clockwork. Co-injections of mRNAs encoding ZFNs targeting the second exon of monarch *cry2* into "one nucleus" stage embryos led to high-frequency nonhomologous end-joining-mediated, mutagenic lesions in the germline (up to 50%). Heritable ZFN-induced lesions in two independent lines produced truncated, nonfunctional CRY2 proteins, resulting in the in vivo disruption of circadian behavior and the molecular clock mechanism. Our work genetically defines CRY2 as an essential transcriptional repressor of the monarch circadian clock and provides a proof of concept for the use of ZFNs for manipulating genes in the monarch butterfly genome. Importantly, this approach could be used in other lepidopterans and "nonmodel" insects, thus opening new avenues to decipher the molecular underpinnings of a variety of biological processes.

[Supplemental material is available for this article.]

The eastern North American monarch butterfly (*Danaus plexippus*) is an emerging model for investigating animal clocks, and navigational and migratory mechanisms (Reppert 2006; Reppert et al. 2010). The navigational abilities of monarch butterflies are part of a genetic program that is initiated in migrants, because the butterflies that make the trip south to Mexico each fall are at least two generations removed from the previous generation of fall migrants (Brower 1996). Important progress to decipher the genetic basis behind the remarkable long-distance migration has been the construction of the draft sequence of the monarch genome (Zhan et al. 2011). Yet, the lack of reverse-genetic tools has hampered the study of gene function. We therefore developed a method for gene inactivation in the monarch butterfly using zinc-finger nucleases (ZFNs).

Migrant butterflies use a time-compensated Sun compass for directional information during their long-distance migration (Perez et al. 1997; Mouritsen and Frost 2002; Froy et al. 2003; Heinze and Reppert 2011). The circadian clock time compensates Sun compass output so that migrants can maintain a fixed flight direction throughout the day. The molecular mechanism of the navigationally important circadian clock is distinctive because it uses two different CRY proteins (Zhu et al. 2005). Monarchs have both the type 1 *Drosophila*-like CRY (designated CRY1), which functions as a circadian photoreceptor for the monarch clock, and the type 2 vertebrate-like CRY2 (not found in *Drosophila*). Like that of *Drosophila* and the mouse, the main gear of the monarch molecular clock is an autoregulatory transcriptional feedback loop. In the proposed monarch model (Fig. 1A), the transcription factors CLOCK (CLK) and CYCLE (CYC) form heterodimers that drive the transcription of the *period* (*per*), *timeless* (*tim*), and *cry2* genes. PER, TIM, and CRY2 are translated, form complexes in the cytoplasm, and cycle back into the nucleus, where CRY2 inhibits CLK:CYC-mediated transcription on an ~24-h basis. However, the transcriptional repressive function of monarch CRY2 in the clock mechanism is based solely on its function in cell culture (Zhu et al. 2008). Defining its essential nature for clockwork function in vivo has been challenging because gene silencing by RNA interference has proven to be difficult in lepidopterans (Terenius et al. 2011; A Casselman and S Reppert, unpubl.) and targeted genomic manipulation to knockout genes of unknown phenotypes has been generally lacking in nondrosophilid insects.

Gene-targeting approaches have recently been developed through the use of custom-designed ZFNs to create heritable lesions in a few invertebrate and vertebrate model organisms (Urnov et al. 2010; Carroll 2011). ZFNs are tailor-made restriction endonucleases capable of inducing a site-specific, double-strand DNA break (DSB) at a desired genomic location. At a low frequency, these DSBs are repaired imprecisely by the error-prone nonhomologous end-joining (NHEJ) DNA repair pathway, generating insertions or deletions (indels) at the target site. When a ZFN-induced DSB is directed to the coding sequence of a gene, the in-

[5]**Corresponding authors**
E-mail steven.reppert@umassmed.edu
E-mail christine.merlin@umassmed.edu
Article published online before print. Article, supplemental material, and publication date are at http://www.genome.org/cgi/doi/10.1101/gr.145599.112. Freely available online through the *Genome Research* Open Access option.

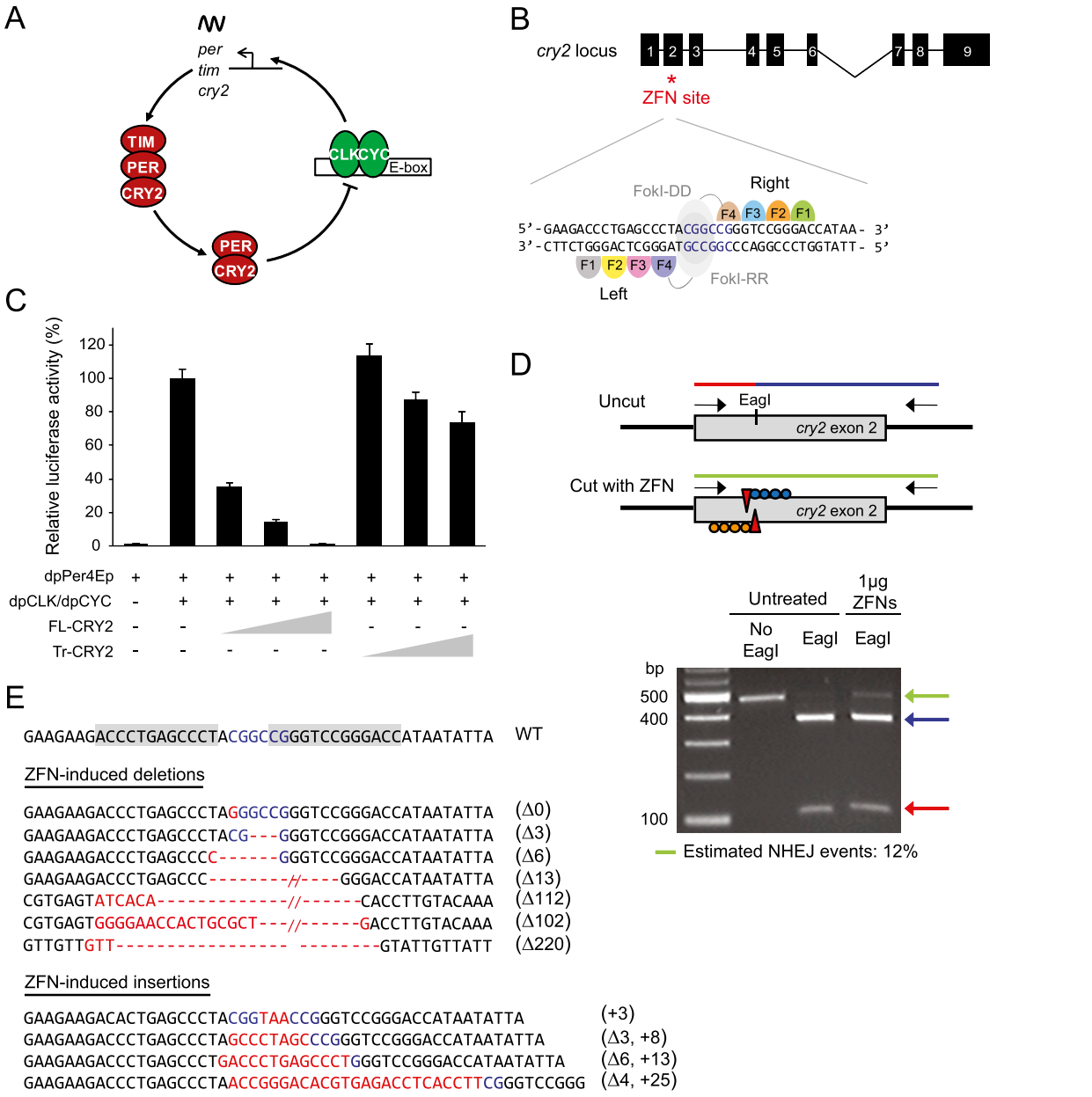

Figure 1. Validation of ZFN activity to target *cry2* in DpN1 cells. (*A*) Proposed core transcriptional feedback loop of the monarch circadian clockwork. CLOCK (CLK) and CYCLE (CYC) heterodimers drive the transcription of *period* (*per*), *timeless* (*tim*), and *cryptochrome 2* (*cry2*), which upon translation form complexes, cycle back into the nucleus, where CRY2 inhibits CLK:CYC-mediated transcription on a 24-h basis. (*B, top*) Schematic of monarch *cry2* gene and position of the ZFN-targeted site (red star). (Black boxes) Exons. (*Bottom*) Magnified view illustrating binding sites for the ZFN pair, each consisting of four zinc-finger modules linked to either DD or RR variants of the FokI endonuclease. (*C*) Wild-type CRY2 (amino acids 1–742) represses CLK/CYC-mediated transcription in S2 cells in a dose-dependent manner, while the truncated protein (amino acids 1–160) does not. The monarch *per* E-box enhancer luciferase reporter (dpPer4Ep; 10 ng) was used in the presence (+) or absence (−) of dpCLK/dpCYC expression plasmids (5 ng each) and either the full-length CRY2 (FL-CRY2; 1, 2, and 10 ng) or truncated CRY2 (Tr-CRY2; 1, 2, and 10 ng). Luciferase activity is relative to beta-galactosidase activity and normalized so that the relative activation by dpCLK/dpCYC alone is 100%. Each value is the mean ± SEM of three independent transfections. (*D, top*) Strategy used to detect ZFN-induced mutations in monarch cells by restriction endonuclease assay. (Red and blue lines) Wild-type genomic amplicon showing the presence of an EagI site. Genomic fragments with mutations induced by NHEJ are resistant to restriction enzyme digestion because of the loss of the EagI site and appear uncleaved (green line). (*Bottom*) Estimation of ZFN activity in DpN1 cells. Genomic amplicons from a pool of cells untreated or treated with 1 µg of ZFNs, subjected to restriction digest. The frequency of NHEJ in treated cells was estimated by quantification of ethidium bromide staining and densitometry of the resistant band (green arrow) relative to wild-type fragments (blue and red arrows). (*E*) ZFN-induced *cry2* mutations in DpN1 cells. (Gray shaded boxes) The ZFN recognition sites on the wild-type sequence. (Blue letters) The EagI site. The positions of (red dashes) deletions and (red letters) insertions.

troduction of mutations can cause frameshifts that lead to the production of null alleles. We therefore developed an approach for high-efficiency targeted mutagenesis in the butterfly germline using ZFNs, focusing on targeting monarch *cry2* to demonstrate feasibility and to further define its role in circadian behavior and the clockwork mechanism in vivo.

Results

Design and in vitro validation of ZFNs targeting *cry2*

Using a computer algorithm, we scanned the monarch *cry2* gene for sequences targetable with our archive of zinc-finger modules (Zhu et al. 2011; Gupta et al. 2012). This analysis identified a high-quality ZFN site in exon 2 comprising two 12-bp zinc-finger recognition elements flanking a 5-bp spacer containing an endogenous restriction site (Fig. 1B). Frameshift mutations at this site are predicted to result in the production of a truncated, nonfunctional protein lacking the structural domains required for its repressive activity in its mammalian counterparts (Chaves et al. 2006). We verified the lack of potent activity of such a truncated monarch CRY2 protein in a transcriptional assay performed in Schneider 2 cells, in which CLK:CYC-mediated *per* transcription is potently inhibited in a dose-dependent manner by full-length CRY2 but only marginally inhibited by the truncated version of the protein (Fig. 1C). We therefore assembled four-finger ZFNs for each recognition element from our archive of zinc-finger modules (Zhu et al. 2011; Gupta et al. 2012) using the obligate heterodimeric RR/DD versions of FokI cleavage domain (Fig. 1B; Miller et al. 2007; Szczepek et al. 2007).

To rapidly assess the efficiency of indel introduction by these ZFNs into the monarch genome, we took advantage of an available monarch cell line (DpN1) (Zhu et al. 2008). We transiently transfected DpN1 cells with different doses of the pair of ZFNs subcloned in an expression vector compatible with DpN1 cells. We used the EagI restriction site present in the spacer between the ZFN binding sites to detect the presence of lesions via the loss of sensitivity of polymerase chain reaction (PCR)–amplified fragments spanning this region to EagI digestion (Fig. 1D, top panel). Complete digestion of the PCR-amplified fragments from untreated DpN1 cells was observed. In contrast, digestion-resistant fragments were found in cells transfected with 1 μg of both ZFNs (as well as other doses tested) (data not shown), consistent with the introduction of lesions at the targeted site (Fig. 1D, bottom panel). We estimated the efficiency of the ZFNs for generating indels at ~12%, which is in the range of previously reported ZFN efficiencies in *Drosophila* embryos (Beumer et al. 2008). To characterize the nature of the *cry2* exon 2 mutations, we cloned and sequenced the resistant PCR fragments from ZFN-treated cells. We obtained a variety of deletions, including microdeletions (3, 6, 13 bp) and larger deletions (102–220 bp), as well as small insertions (Fig. 1E). Sixty-four percent of these indels (7/11) led to a frameshift that should result in a truncated CRY2 protein.

High-efficiency germline targeting by injections into 'one nucleus' embryos

To generate monarch CRY2 knockouts, we established a delivery technique to efficiently and reproducibly target the germline precursors in vivo by injecting capped mRNA encoding the ZFNs into fertilized eggs at the "one nucleus" stage (Fig. 2). In contrast to *Drosophila* and *Bombyx*, the precise location of germline precursor cells within the developing monarch embryo is unknown. However, it is known in lepidopterans, as in many other insects, that sperm stored in the spermatheca of the female is transferred into the egg for fertilization at oviposition through a micropylar orifice present at the anterior pole of the egg (Kobayashi et al. 2003). It has been reported that both the male and female pronucleus form in this region in lepidopterans, before slightly migrating toward the center of the egg, where they unite in the zygote nucleus and start mitotic divisions. These divisions give rise to numerous cleavage nuclei that migrate toward the egg periphery to form the syncytial blastoderm. At this stage, primordial germ cells form in the posterior region of the egg (Kobayashi et al. 2003). We reasoned that injecting the ZFN mRNAs just after fertilization in the anterior region of the egg close to the micropyle would favor the production of indels in the genome that could be transmitted through the germline with high frequency, because the targeting would occur at a stage of development that contains a minimal number of nuclei.

After injections of both ZFNs into embryos at two different concentrations (0.5 and 0.1 μg/μL), we observed a low hatching rate (from ~2% to ~5%) (Table 1), which increased with decreasing doses of ZFNs (Table 1), suggesting dose-dependent toxicity of the ZFNs. Embryo injections of an equivalent amount of mRNA encoding either of the ZFN monomers led to an increase in hatching rate, indicating that some of the toxicity observed was due to off-target cleavage by the pair of heterodimeric ZFNs (Fig. 3A), as previously reported in other systems (Porteus and Baltimore 2003; Alwin et al. 2005; Cornu et al. 2008; Meng et al. 2008; Gupta et al. 2011). In addition, we also observed a near fourfold decrease in hatching rate between uninjected eggs and embryos injected with water (from ~75% to ~20% hatching), suggesting that the injection procedure contributes, together with the toxicity of the ZFNs, to the low survival of injected embryos. The sensitive location of the injection may, indeed, represent a major factor causing embryonic lethality through either dehydration via the punctured chorion and/or mechanical damage, such as displacement or loss of the first nuclei.

Nevertheless, the technique enabled high-frequency targeted mutagenesis in both somatic cells (Fig. 3B,C) and germline cells (see below). PCR-based genotyping of embryos injected with both ZFNs that failed to complete development revealed somatic mutations in 44% (30/68) to 88% (50/57) of these animals depending on the ZFN dose injected (Table 1), with rates of indels ranging from a few percent to full targeting, based on the relative intensity of digestion-resistant fragments (Supplemental Fig. S1A). Importantly, the presence of somatic mutations, tested using noninvasive genotyping techniques (see Fig. 2), was found in ~3% to ~9% of the screened live larvae, at a frequency estimated from ~9% to ~55% (Fig. 4A; Supplemental Fig. S1B; Table 1).

To determine whether ZFN-induced mutations could be transmitted through the monarch germline, we reared the four viable larvae that exhibited somatic mosaicism from the 0.1 μg/μL ZFN dose (Supplemental Fig. S1B) on a semi-artificial diet. Larvae were raised to adulthood and backcrossed to wild-type adults. Of note, we could not assess germline targeting in the two somatic larvae generated from injections at 0.5 μg/μL of ZFNs because they died before reaching adulthood (Table 1). Out of the four putative founders, three produced progeny at a rate similar to uninjected animals (Fig. 4A, males #1–#3). We screened 658 G_1 progeny for the presence of mutations and recovered 125 mutants. These mutants were found in the progeny of two male founders, each generated from an independent set of injections, that produced germline mutants in 50% and 39.2% of their progeny (Fig. 4A). This represents a germline targeting efficiency comparable to that of *Drosophila* and the cricket (Beumer et al. 2008; Watanabe et al. 2012) and is two orders of magnitude higher than that previously reported in *Bombyx* (Takasu et al. 2010). This increased efficiency in lepidopterans might reflect the importance of injecting eggs at the "one nucleus" stage to attain reproducible, high-efficiency germline targeting in these species.

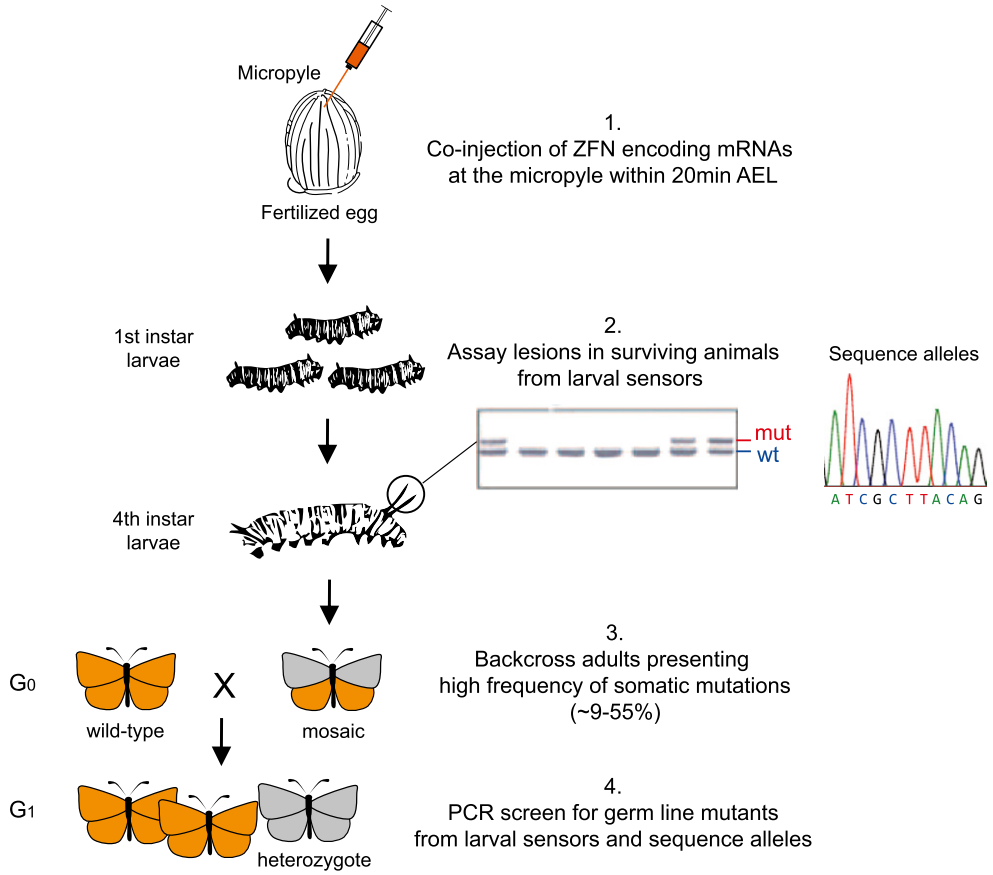

Figure 2. Injection and screening strategy for recovering germline-transmitted ZFN-induced mutants. (1) To target the first nuclei during embryonic development, fertilized eggs are injected with ZFN-encoding mRNAs within 20 min after egg laying (AEL) at the micropyle, the region at which the sperm is transferred and fertilization occurs in holometabolous insects. (2) Surviving larvae are reared to the fourth instar larvae and then are subjected to noninvasive genotyping to screen for mosaics presenting a high frequency of targeting in somatic cells. The presence of lesions is tested by restriction endonuclease assay from fleshy filaments of a single animal (larval sensors at the anterior thorax) whose removal does not alter the butterfly's survival or fertility, and the mutated alleles are sequenced. Of note, for species that do not possess external structures, genotyping could alternatively be performed using hemolymph extracts. (3) To reduce breeding efforts, only mosaic larvae targeted with high frequency in somatic cells are reared to adulthood (mixed orange and gray) and backcrossed to wild-type butterflies (orange). (4) The G_1 progeny are screened for targeted mutations as in 2.

Characterization of germline transmitted ZFN-mediated mutations

To characterize the nature of the ZFN-induced germline mutations, we cloned and sequenced the PCR fragments corresponding to the mutated alleles from each progeny (Fig. 2). We recovered a single mutation at the targeted sequence transmitted by each founder, with one having a 4-bp deletion and the other a 2-bp insertion. Both mutations caused a frameshift that would result in truncated CRY2 proteins (Fig. 4A,B). Interestingly, each mutation was identical to the one detected in somatic cells of either founder (data not shown). This not only indicates that all heterozygous animals originated from germline precursor cells carrying the same mutation but also supports our hypothesis that the features (time and location) of our delivery technique favor targeting at the "one nucleus" stage during development. By crossing sibling heterozygous for each mutation, we generated two independent *cry2* mutant butterfly lines. We verified that both mutations lead to the production of truncated proteins by Western blot analysis of brain tissue of wild-type, heterozygous, and homozygous mutants, using a monarch-specific anti-CRY2 antibody directed against the C terminus of the protein (Fig. 4C; Supplemental Fig. S2). Predictably, we did not detect any signal at the expected size of full-length CRY2 in the brains of either knockout butterfly line (Fig. 4C).

Targeted mutagenesis of *cry2* disrupts the circadian clockwork

To assess the effect of monarch CRY2 knockouts on circadian behavior, we examined the time of day of adult eclosion (the emergence of the adult butterfly from its chrysalis) (Fig. 5A), a robust and easily tractable behavior that is restricted to the early portion of the light period in monarchs and whose time-of-day occurrence is under circadian control (Froy et al. 2003). We examined the two independent lines generated to exclude any off-target effects on the behavior. For study of the timing of eclosion, monarchs were entrained in 15-h light:9-h dark (LD) cycles throughout their larval and pupal stages and placed into constant darkness (DD) a day or two prior to the expected time of eclosion. We found that the circadian timing of adult eclosion in DD was disrupted in both knockout lines, while sibling-matched wild-type and heterozygote animals exhibited normal eclosion timing (Fig. 5B; one-way ANOVA, $P < 0.0001$ for both lines; see also Supplemental Fig. S3).

To examine how the molecular clock was altered in CRY2 knockout butterflies, we quantified by quantitative real-time PCR

Table 1. Injection data of ZFN-mediated targeted mutagenesis at the *cry2* locus at two doses of ZFN mRNAs

Concentration ZFNs	0.5 μg/μL	0.1 μg/μL
Embryos injected, *n*	4189	1194
Developing embryos at day 2, *n*	168	114
Dead embryos at day 4, *n*	68	57
Somatic mosaics from dead embryos at day 4, *n* (%)	30/68 (44.1%)	50/57 (87.7%)
Hatched larvae, *n* (%)	100 (2.38%)	57 (4.8%)
Dead larvae, *n*	31	12
Somatic mosaics from dead larvae, *n* (%)	5/31 (16.1%)	2/12 (16.6%)
Live larvae, *n*	69	45
Somatic mosaics from live larvae, *n* (%)	2/69 (2.9%)	4/45 (8.9%)
Live somatic adult, *n*	0	4
Founders	—	2

For each concentration of ZFN mRNAs injected, the total number of embryos injected, the number of embryos developing at day 2 (i.e., at the mid-period of embryonic development), the number of hatched larvae, and the percentage relative to the number of embryos injected are shown; and the number of surviving larvae and somatic adults are shown. Among the developing embryos and hatched larvae, a portion died during embryonic developmental or at the larval stage while other survived. All of these embryos and larvae (dead embryos, dead larvae, live larvae) were subjected to a restriction endonuclease assay, and the number and percentage of somatic mosaics from each group are shown. The number of targeted animals reaching adulthood and those carrying mutations in the germline (founders) are reported.

the expression of the clock genes *period* (*per*) and *timeless* (*tim*) from both brains and antennae, major sites of circadian clocks in the monarch (Zhu et al. 2008; Merlin et al. 2009), in wild-type, heterozygous, and homozygous butterflies carrying the 4-bp deletion mutation (Fig. 6A). We performed our analysis during the first day of DD after entrainment to LD for 7 d. While *per* and *tim* exhibited robust circadian rhythms in both tissues of wild-type and heterozygous butterflies, their rhythmic expression was abolished in the homozygous CRY2 knockouts; there was constitutive high expression in brains and a lack of significant expression cycling in antennae (Fig. 6A; two-way ANOVA, interaction genotype × time: *per* in brain and antenna, $P < 0.0001$, *tim* in brain, $P < 0.005$, *tim* in antenna, $P < 0.0001$; one-way ANOVA for antennae; *per*, $P = 0.19$, *tim*, $P = 0.065$). Significantly higher expression levels of *per* and *tim* were also found in the brains and antennae of 2-bp insertion CRY2 knockouts, compared with the low mRNA levels exhibited by these genes at CT12 (the trough) in sibling wild-type and heterozygous butterflies (Fig. 6B; Student's *t*-test, $P < 0.05$ for *per* and *tim*). Together, these results demonstrate that monarch CRY2 functions in vivo as the major transcriptional repressor of both the central and peripheral clock feedback loops, in line with its proposed function in the nondrosophilid insect clockwork (Yuan et al. 2007; Zhu et al. 2008; Ikeno et al. 2011a,b).

Discussion

Although ZFNs have emerged as powerful tools for precise genome manipulation in insects (Bibikova et al. 2002; Beumer et al. 2006, 2008; Takasu et al. 2010; Watanabe et al. 2012), achieving efficient nuclease-mediated germline targeted mutagenesis in nondrosophilid insects has been challenging. Recently, Watanabe et al. (2012) reported nuclease-mediated targeted mutagenesis in a hemimetabolous insect, with efficiencies comparable to that observed in *Drosophila*. Here, we provide a timely demonstration that high-efficiency ZFN-mediated germline targeting can also be attained in the butterfly, a holometabolous insect, by using ZFNs, along with an improved nuclease-delivery approach into the embryo. Compared with the low germline transmission efficiency described for targeted mutagenesis of epidermal marker genes in *Bombyx* (0.28%; 46 transformants out of 16,350 offspring) (Takasu et al. 2010), our approach in the monarch butterfly permits an overall germline targeting rate of ~19% (125 transformants out of 658 offspring), which can reach 50% in the progeny of a single founder. This substantial increase of germline transmission rate in lepidopterans may result from the combined action of dosage optimization of ZFNs to maximize survival among targeted animals, and our delivery and screening strategy.

Delivering nucleases at the "one nucleus" stage in the embryo offers several advantages over classical approaches used in lepidopterans, in which material is commonly delivered at the syncytial preblastoderm stage and at the posterior pole of the egg (Peloquin et al. 2000; Tamura et al. 2000; Marcus et al. 2004; Takasu et al. 2010), when many cleavage nuclei are present. One advantage of our delivery system is that it circumvents the need to define the location of germ cell precursors during embryonic development in species for which development remains poorly characterized. In addition, injecting the embryo at the "one nucleus" stage bypasses the difficulty of mRNA incorporation into germ cell precursors in lepidopterans, proposed as a potential cause of the low efficiency of germline targeting in *Bombyx* (Takasu et al. 2010). Finally, by inducing high-frequency mutations in both the germline and somatic cells, the strategy facilitates the selection of candidate founder animals on the basis of high-frequency targeting in somatic cells. Indeed, two out of four selected potential founders targeted with a frequency approximating 50% in somatic cells produced mutants in 39%–50% of their progeny in our study. The lack of germline-transmitted mutations in the progeny of the other two animals, targeted at 9% and 28% in somatic cells, suggests that targeting can also occur after the first nucleus division. The selection step introduced in our approach is important because it reduces costly and time-consuming high-throughput breeding and screening efforts. Such a selection was not achievable with previously described methods designed to preferentially target the germline precursor cells in *Drosophila*, *Bombyx*, or the cricket (Beumer et al. 2008; Takasu et al. 2010; Watanabe et al. 2012). Because early embryonic development is largely conserved in lepidopterans (Kobayashi et al. 2003) and the micropyle is easy to locate, the application of our nuclease-mediated targeted mutagenesis approach should represent a practical technique by which the broad community working on a variety of moths and butterflies could develop reverse genetics in their species of choice.

It is worth noting that even though we used an endogenous restriction site at the ZFN target site, which makes ZFN-induced mutations easily detectable, most quality ZFN sites found in a given genome do not contain suitable restriction sites for rapid genotyping. In which case, one can alternatively detect the presence of mutations at loci of interest by using a mismatch-sensitive nuclease (Cel-I or T7E1) assay (Kim et al. 2009; Guschin et al. 2010). The primary caveat when using these assays is their sensitivity to SNPs, which necessitates the use of uninjected sibling animals as negative controls.

Using the ZFN technology, we generated, to our knowledge, the first insect knockout of an unknown phenotype (i.e., not visually tractable) based solely on molecular assays. This allowed us

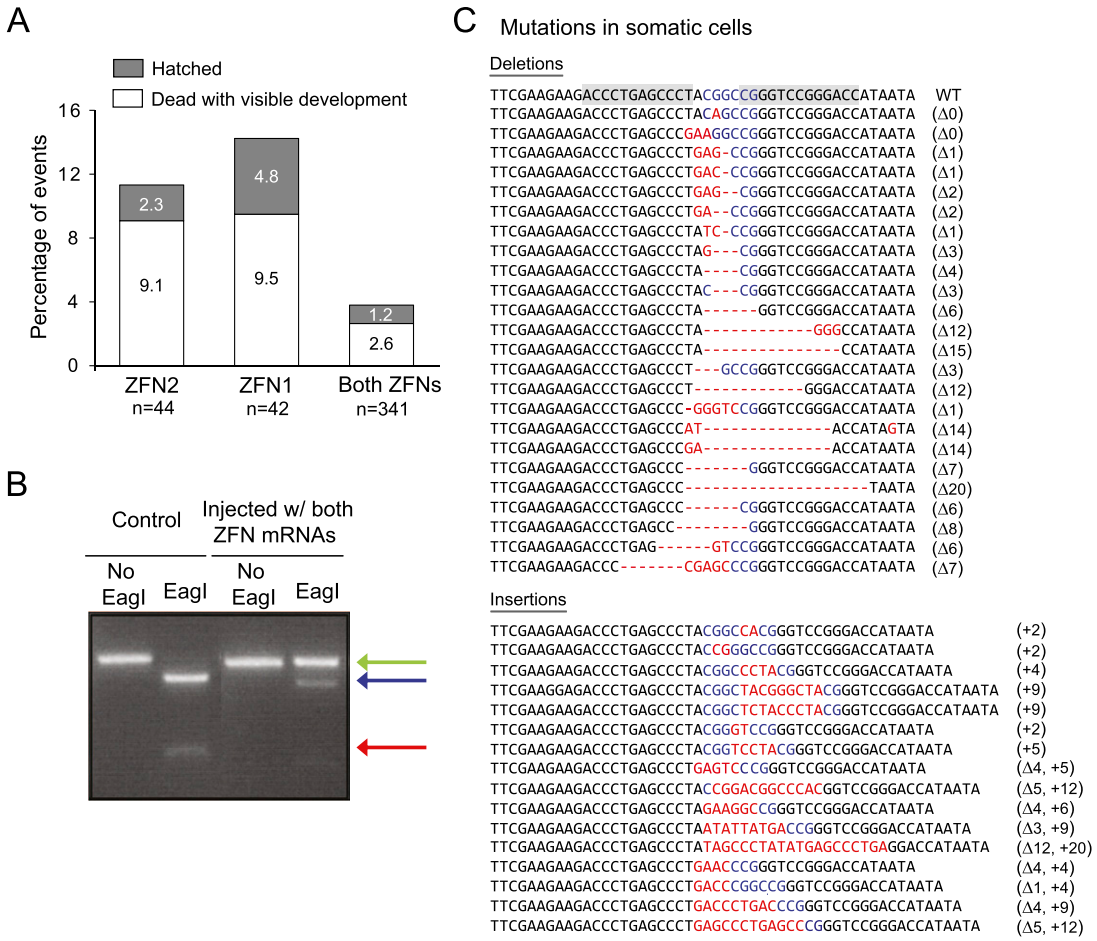

Figure 3. ZFN-induced mutagenesis at the *cry2* locus in somatic cells. (*A*) Effects of ZFN mRNA injections on monarch embryos. The bar graph depicts the rate of hatching larvae (gray bars) and of embryos presenting development but dying before hatching (white bars), associated with egg injection of each of the ZFNs mRNA alone (linked to either of the obligate heterodimeric versions of the FokI nuclease domain) or both ZFNs mRNA at 0.5 μg/μL. For comparison, control embryos injected with water in similar conditions hatch at a rate of 19.5% with an additional 3.6% that develop but die before hatching ($n = 82$). Uninjected embryos hatch at a rate of ~75%. (*B*) Agarose gel example of lesions observed in somatic cells of hatched larvae and dead embryos injected with both ZFN mRNAs, showing a high degree of targeting (green arrow), compared with an uninjected control. (*C*) Mutations observed in somatic cells of dead embryos, and dead or live larvae, from eggs injected at different doses of ZFN mRNAs.

to demonstrate the applicability of our ZFN approach to study the genetic basis of a complex behavioral phenotype. As a result, we have genetically defined the essential function of insect CRY2 in the central and peripheral clockwork mechanism as the major transcriptional repressor of CLK:CYC-mediated transcription, as suggested by previous studies (Ikeno et al. 2011a,b). Because insect CRY2 is not found in *Drosophilae*, our study highlights the importance of genetic manipulation for understanding circadian clock mechanisms in nondrosophilid insect species. In addition, monarch CRY2 knockouts represent a valuable resource to further study the involvement of the circadian clock in monarch butterfly migration, such as CRY2's role in the initiation of the migratory state (Reppert et al. 2010).

Targeted mutagenesis approaches in the monarch butterfly, in combination with the draft sequence of its genome (Zhan et al. 2011), open new avenues of investigation into the molecular mechanisms underlying migratory behaviors. Given the variability of gene silencing by RNAi approaches in lepidopterans (Terenius et al. 2011), the application of similar nuclease-based approaches to other species could greatly enhance both basic and applied science. In butterflies such as *Heliconius* and *Bicyclus*, which are model systems in evolutionary biology (Beldade et al. 2008; The *Heliconius* Genome Consortium 2012), reverse genetics could advance the dissection of the genetic and developmental mechanisms of organismal diversity, e.g., speciation. In addition, because some species of moths, such as species from the genus *Helicoverpa* (Downes et al. 2007), are crop pests of economic importance worldwide, reverse-genetic approaches in these species could improve effective pest control. The further development of nuclease-based reverse-genetic approaches in "nonmodel" insects is important because of the forthcoming explosion of insect genome sequencing projects (Robinson et al. 2011) and will be facilitated by the continued improvements in the activity and precision of both ZFNs (Carroll 2011) and transcription activator-like effector nucleases (TALENs) (Mussolino and Cathomen 2012). Moreover, these reverse-genetic strategies, which will invariably include tissue/temporal conditional alleles, should accelerate the dissection of a variety of biological processes, e.g., the genetic basis of migration, for which the use of *Drosophila* is not well suited.

A

Founders sex	#	Fertile	Mosaicism, %	Progeny, n	Mut/parent, n	Mut/total , %	Mutation type, n
Female	#1	yes	~9	21	0	-	-
Male	#1	yes	~50	86	43	50	1 (M1)
	#2	yes	~55	209	82	39.2	1 (M2)
	#3	yes	~28	342	0	-	-

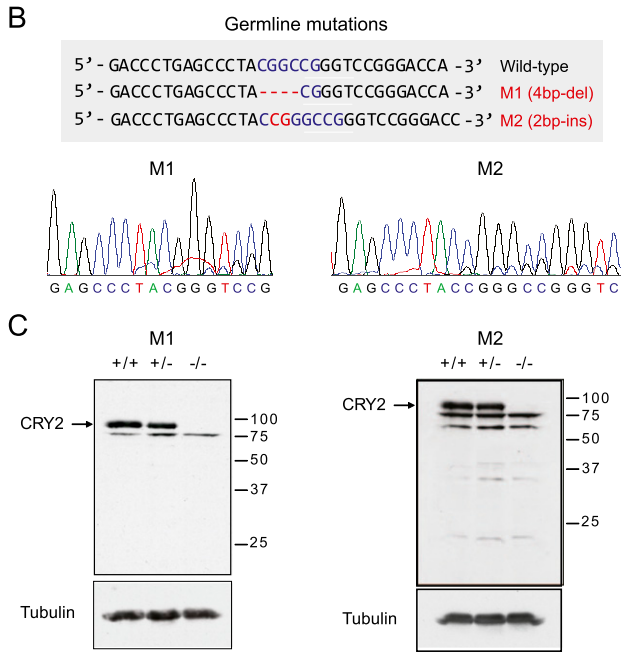

Figure 4. Germline transmission of *cry2* ZFN-targeted mutations. (*A*) Table of heritable NHEJ mutagenesis at the *cry2* locus. Potential founders (sex and number) presenting a high level of targeting in somatic cells that produced fertile crosses and those that yielded mutant progeny are shown. The approximate level of mosaicism, the number of progeny screened, the number of mutants per parent, the percentage of mutants in the progeny of each founder, and the number and name of mutations recovered are reported. The level of mosaicism was estimated by quantification of ethidium bromide staining and densitometry of the resistant band relative to wild-type fragments. (*B*) Alleles carried by founders showing mutations at the targeted site, a 4-bp deletion (M1) and a 2-bp insertion (M2), respectively, transmitted to 50% and 39.2% of the offspring (see above). Both mutations cause frameshifts leading to truncated proteins. (*Top*) Sequences; (*bottom*) chromatogram profiles. (*C*) Western blot analyses of CRY2 in brains of sibling wild-types (+/+), and heterozygous (+/−) and homozygous (−/−) mutants for each mutation. (*Left*) Four-base-pair deletion (M1); (*right*) 2-bp insertion (M2). The specific band recognized by a monarch-specific anti-CRY2 antibody directed against the C terminus of the protein (lacking in homozygous mutants) is identified by the arrow on the *left* of each panel.

Methods

Butterfly husbandry

Monarch butterflies originating from reproductive monarchs captured in the wild in Kansas were maintained in the laboratory. Egg laying was performed on milkweed (*Asclepias curassavica*), their obligate host plant. First to second instar larvae were transferred with a small paintbrush onto a semi-artificial diet and reared individually in Percival incubators at 25°C, 50% humidity, and under 15-h light:9-h dark (LD) conditions. Adult monarchs were housed in glassine envelopes and fed a 25% honey solution daily.

Target selection and ZFN assembly

Potential ZFN target sites within the monarch *cry2* coding exons were identified using a computational algorithm that identifies sequences compatible with our archive of one-finger (Zhu et al. 2011) and two-finger modules (Gupta et al. 2012) and scores the quality of these sequences. A favorable ZFN target site, gACCCTGAGCCCT acggcCGGGTCCGGGACc, was identified within exon 2 of *cry2*. Two four-finger arrays were constructed for each subsite by PCR assembly from our finger archives as previously described (Supplemental Table S1; Gupta et al. 2012). The sequences of these zinc-finger arrays were cloned into pCS2 vectors containing the DD (R487D) and RR (D483R) obligate heterodimeric versions of the FokI nuclease domain (Miller et al. 2007; Szczepek et al. 2007), a nuclear localization signal and an epitope tag (either Flag- or HA-tag, respectively).

ZFN sites density analysis in monarch coding exons

The number of ZFN target sites within the coding exons of the monarch genome (http://monarchbase.umassmed.edu/) (Zhan et al. 2011) was assessed based on the available archives of single-finger

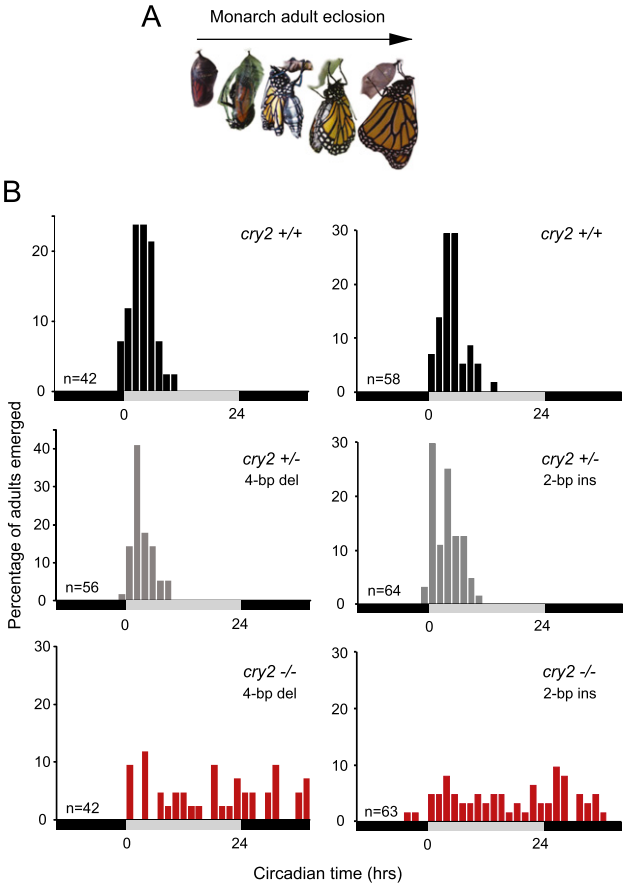

Figure 5. CRY2 deficiency disrupts circadian behavior. (*A*) The act of monarch eclosion from chrysalis to butterfly. (*B*) Profiles of adult eclosion in constant darkness (DD) of wild-type (+/+, black), heterozygous (+/−, gray), and homozygous mutant (−/−, red) siblings of the 4-bp deletion (*left*) and the 2-bp insertion (*right*) *cry2* mutant line, entrained to LD throughout their larval and pupal stages. Eclosion occurred on the first day and second day of DD. Data from both days are pooled and binned in 1-h intervals (for detailed data throughout the 2 d in DD) (see Supplemental Fig. S3). Effect of genotype on eclosion time, one-way ANOVA: $P < 0.0001$ for both lines; Tukey post-hoc test: +/+ versus +/−, $P > 0.05$; +/+ versus −/−, $P < 0.01$; +/− versus −/−, $P < 0.01$ for both lines. (Black horizontal bars) Night/subjective night; (gray horizontal bars) subjective day.

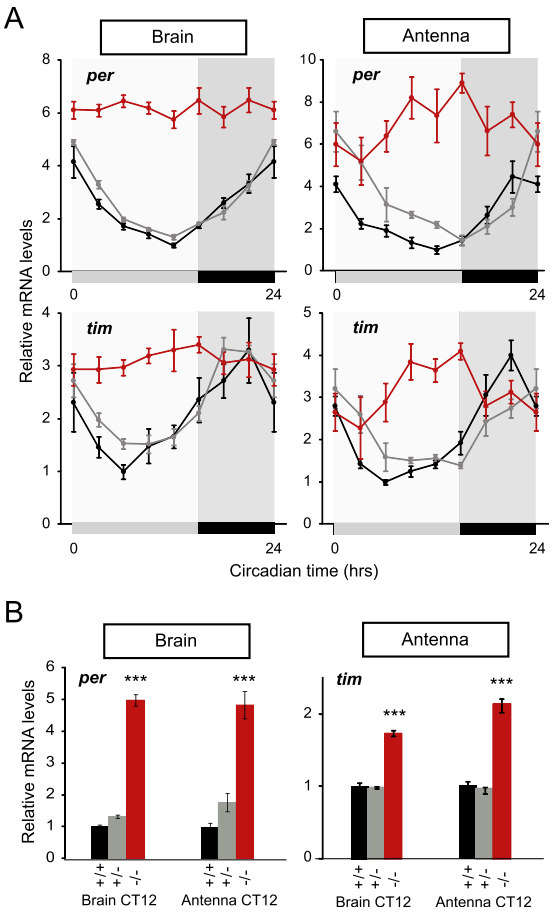

Figure 6. CRY2 deficiency disrupts the molecular clockwork. (*A*) Circadian expression of *per* and *tim* in brains and antennae of adult wild-type in constant darkness (DD) of wild-type (black lines), heterozygous (gray lines), and homozygous mutant (red lines) siblings of the 4-bp deletion *cry2* mutant line entrained to LD throughout their larval and pupal stages. Values are mean ± SEM of four animals. Interaction genotype × time, two-way ANOVA: *per* in brain, $P < 0.0001$; *per* in antenna, $P < 0.0001$; *tim* in brain, $P < 0.005$; *tim* in antenna, $P < 0.0001$. (Box shading: light gray) Subjective day; (dark gray) night. (*B*) Expression levels of *per* and *tim* in brains and antennae of adult from the three genotypes of the 2-bp insertion *cry2* mutant line at circadian time (CT)12, which corresponds to the trough of *per* and *tim* rhythmic expression in wild type. One-way ANOVA: $P < 0.0001$ for *per* and *tim* in both tissues; post-hoc *t*-test: $P < 0.05$ for *per* and *tim* between wild-type and knockouts, and heterozygotes and knockouts in both tissues. Values are the mean ± SEM of six animals. (Black bars) Wild type (+/+); (gray bars) heterozygous mutants (+/−); (red bars) homozygous mutants (−/−).

(Zhu et al. 2011) and two-finger modules (Gupta et al. 2012) that can be assembled into three- or four-fingered ZFNs. A Perl script was used to define all of the sequences compatible with the ZFNs constructed from these archives allowing a 5-bp, 6-bp, or 7-bp gap between the recognition sites of the two monomers comprising a functional dimer. The output of this analysis provided the number of unique ZFN sites within each gene (or the absence thereof) for the 16,866 annotated unique genes within the genome. Overall, 179,590 ZFN sites were found, with 15,301 unique genes hit by at least one ZFN and an average number of ~10.6 ZFN sites per gene.

Preparation of ZFN mRNA

pCS2-ZFN constructs were linearized with NotI, extracted with phenol:chloroform, and precipitated with ethanol and sodium acetate. mRNA was in vitro–transcribed using the mMessage mMachine SP6 kit (Ambion) and polyadenylated using the Poly(A) Tailing Kit (Ambion), according to the manufacturer's instructions. The resulting capped poly(A) mRNA was purified by phenol: chloroform extraction followed by isopropanol precipitation; the precipitate was resuspended in RNase-free water. mRNAs encoding the *cry2* ZFNs were quantitated using a Nanodrop-2000c (Thermo Scientific), diluted in RNase-free water and mixed to a final concentration of 0.5 μg/μL and 0.1 μg/μL, and stored at −80°C until use.

Egg microinjection

Eggs were collected from milkweed leaves following 10-min oviposition bouts, aligned on thin strips of double-sided adhesive tape onto microscope slides, and placed into plastic Petri dishes. Eggs were injected through the chorion under a dissecting microscope, using a pulled borosilicate glass needle attached to a Pneumatic Picopump microinjection apparatus (World Precision Instruments), within 20 min after egg laying at the anterior pole, which corresponds to the putative region and time frame of the first mitotic divisions (i.e., at "one nucleus" stage). After injection, embryos were placed in an incubator at 25°C and 70% relative humidity with extra moisture inside the dishes. Embryos that displayed signs of development at day 2 under microscope observation were transferred into individual small Petri dishes until larvae hatched 4–5 d later. Larvae were fed milkweed leaves until the second larval instar, when they were transferred onto semi-artificial diet and reared until the fourth instar.

Screening strategy

Surviving fourth instar larvae were screened for the presence of mutations at the targeted site by noninvasive genotyping, using cuticular expansions at the anterior of their thorax (larval sensors), whose removal did not alter the butterfly's survival or fertility and from which enough DNA could be obtained for PCR amplification. Larvae presenting a high degree of targeting in somatic cells were selected for further analysis and reared to adulthood. Adults were mated in individual cages with several virgin wild-type individuals of the opposite sex to establish lines. Eggs were collected from each line, and the larvae were raised and screened for the presence of mutated alleles as described above.

Cell culture, transfections, and transcriptional assay

DpN1 cells were cultured and transfected as previously described (Zhu et al. 2008). DpN1 cell expression constructs were generated by subcloning into pBA the cassette encoding the nuclear localization signal, epitope tag, each zinc-finger protein, and its associated FoKI cleavage domain variant using the primers pCS2_F (5′-ATGCGGCCGCATGGCTCCAAAGAAGAAGCG-3′) and PCS2_R (5′-CGCCTCGAGTTAAAAGTTTATCTCGCCGT-3′).

Schneider 2 (S2) cells were cultured and transfected to perform transcriptional assays as previously described (Chang and Reppert 2003), using the S2 cell expression constructs generated previously (Zhu et al. 2005; Yuan et al. 2007), except for the deleted monarch CRY2 construct lacking the 582 C-terminal amino acids. This construct was generated by subcloning into the pAc5.1V5/HisA vector (Invitrogen) a truncated version of CRY2 amplified using the primers trCry2_F (5′-CGGGTACCATGTCGGTTGCCGAGA-3′) and trCry2_R (5′-GCTCTAGAGTAGGGCTCAGGGTCTTC-3′).

Sequence analysis of ZFN-induced mutations

Genomic DNA from DpN1 cells or larval sensors was extracted using 0.01× proteinase K in lysis buffer (100 mM Tris at pH 8.0, 200 mM

NaCl, 5 mM EDTA, 0.2% SDS). Fragments flanking the targeted region in DpN1 cells and larval sensors (of 467 bp and 528 bp, respectively) were amplified by PCR using the primers *cry2*_F2 (5′-ATTCGTGGTGAGAGGTCAGC-3′) and *cry2*_R2 (5′-GTGTCGGCAC TCCAAATCTT-3′) in DpN1 cells, and *cry2*_F1 (5′-ATTCCCGTTTA TTCGTGGTG-3′) and *cry2*_R4 (5′-AATATAACGAGGGCATAGCT-3′) in larval sensors, and subjected to restriction fragment length polymorphism analysis using EagI. Fragments corresponding to mutated alleles were gel-purified, cloned, and sequenced, or directly sequenced, using the same primers.

Eclosion behavior

Monarch larvae were housed in LD in a Percival incubator at 25°C and 50% humidity through pupation. One to two days prior to adult eclosion, the pupae were transferred to constant darkness (DD). Eclosion behavior was monitored continuously over 2 d using infrared security cameras (Swann Pro-550/560/580) mounted inside the incubator and recorded with a digital video recorder (8ch H.264 DVR; Swann). Eclosion data were analyzed and plotted as 1-h bins.

Tissue collection

For RNA extractions, brains (free from eye photoreceptors) and antennae were dissected in DD under infrared illumination every 3 h over 24 h from butterflies entrained in LD for 7 d prior to dissection, and stored at −80°C until use. Brain dissections were performed in 0.5× RNA later (Ambion) to avoid RNA degradation. For protein extractions, brains were dissected in 1× Ringer's solution.

Western blotting

Western blots of brain and S2 cell extracts were probed with the primary antibody guinea pig anti-CRY2.51 (1:3000) (Zhu et al. 2008), a monoclonal mouse anti-α-tubulin (1:40,000), and a monoclonal anti-V5 IgG antibody (Invitrogen). Secondary antibodies were horseradish peroxidase–conjugated donkey anti-guinea pig IgG (Jackson Immunoresearch Laboratories; 1:10,000) and horseradish peroxidase–conjugated goat anti-mouse IgG (Santa Cruz; 1:32,000). Western blotting was performed as described previously (Lee et al. 2001; Zhu et al. 2008).

Quantitative real-time PCR

Total RNA was processed from single brain or antenna as previously described (Merlin et al. 2009). The quantifications of clock gene expression were performed using real-time quantitative PCR by TaqMan probes with an ABI Prism 7000 SDS (Applied Biosystems). The monarch *per*, *tim*, and control *rp49* primers and probes were identical to those reported previously (Zhu et al. 2008). PCR amplification and data analyses were performed as previously described (Merlin et al. 2009). For temporal profiling experiments, the values for each gene in a given tissue were normalized to *rp49* as an internal control and normalized to the lowest expression level of all genotypes. For differences of gene expression levels between genotypes at a single time point (CT12), the values for each gene in a given tissue were normalized to *rp49* and normalized to the wild-type value.

Statistical analysis

P-values were calculated using a Student's *t*-test and one-way and two-way ANOVA, calculated by GraphPad Prism version 5.

Acknowledgments

We thank Daniel Newman and Andrew Dowd for technical help; Amy Rayla and Ankit Gupta for zinc-finger assembly assistance; Sriramana Kanginakudru for initial work on this project; Ann Ryan for diet and monarch butterflies; Antonia Monteiro for egg injection advice; and Robert Agate, Jerome Menet, Patrick Emery, and members of the Reppert laboratory for discussions. This work was supported by NIH grant R01 GM086794 to S.M.R. and R01 GM068110 to S.A.W. C.M. is supported by a Charles A. King Trust Postdoctoral Fellowship, Bank of America, N.A., Co-Trustee. The funders had no role in study design, data collection and analysis, decision to publish, or preparation of the manuscript.

Authors' contributions: S.M.R. initiated and oversaw the project. C.M., S.A.W., and S.M.R. conceived the ZFN strategy for targeted mutagenesis in monarch butterflies. S.A.W. designed the ZFNs and guided their use. C.M. developed the egg microinjection and screening strategy, and performed all the experiments. L.E.B. helped with husbandry and genotyping. O.R.T. provided the semi-artificial diet and husbandry guidance. C.M., L.E.B., S.A.W., and S.M.R. performed data analyses. C.M., S.A.W., and S.M.R. wrote the paper.

References

Alwin S, Gere MB, Guhl E, Effertz K, Barbas CF III, Segal DJ, Weitzman MD, Cathomen T. 2005. Custom zinc-finger nucleases for use in human cells. *Mol Ther* **12:** 610–617.

Beldade P, McMillan WO, Papanicolaou A. 2008. Butterfly genomics eclosing. *Heredity* **100:** 150–157.

Beumer K, Bhattacharyya G, Bibikova M, Trautman JK, Carroll D. 2006. Efficient gene targeting in *Drosophila* with zinc-finger nucleases. *Genetics* **172:** 2391–2403.

Beumer KJ, Trautman JK, Bozas A, Liu JL, Rutter J, Gall JG, Carroll D. 2008. Efficient gene targeting in *Drosophila* by direct embryo injection with zinc-finger nucleases. *Proc Natl Acad Sci* **105:** 19821–19826.

Bibikova M, Golic M, Golic KG, Carroll D. 2002. Targeted chromosomal cleavage and mutagenesis in *Drosophila* using zinc-finger nucleases. *Genetics* **161:** 1169–1175.

Brower LP. 1996. Monarch butterfly orientation: Missing pieces of a magnificent puzzle. *J Exp Biol* **199:** 93–103.

Carroll D. 2011. Genome engineering with zinc-finger nucleases. *Genetics* **188:** 773–782.

Chang DC, Reppert SM. 2003. A novel C-terminal domain of *Drosophila* PERIOD inhibits dCLOCK:CYCLE-mediated transcription. *Curr Biol* **13:** 758–762.

Chaves I, Yagita K, Barnhoorn S, Okamura H, van der Horst GT, Tamanini F. 2006. Functional evolution of the photolyase/cryptochrome protein family: Importance of the C terminus of mammalian CRY1 for circadian core oscillator performance. *Mol Cell Biol* **26:** 1743–1753.

Cornu TI, Thibodeau-Beganny S, Guhl E, Alwin S, Eichtinger M, Joung JK, Cathomen T. 2008. DNA-binding specificity is a major determinant of the activity and toxicity of zinc-finger nucleases. *Mol Ther* **16:** 352–358.

Downes S, Mahon R, Olsen K. 2007. Monitoring and adaptive resistance management in Australia for Bt-cotton: Current status and future challenges. *J Invertebr Pathol* **95:** 208–213.

Froy O, Gotter AL, Casselman AL, Reppert SM. 2003. Illuminating the circadian clock in monarch butterfly migration. *Science* **300:** 1303–1305.

Gupta A, Meng X, Zhu LJ, Lawson ND, Wolfe SA. 2011. Zinc finger protein-dependent and -independent contributions to the in vivo off-target activity of zinc finger nucleases. *Nucleic Acids Res* **39:** 381–392.

Gupta A, Christensen RG, Rayla AL, Lakshmanan A, Stormo GD, Wolfe SA. 2012. An optimized two-finger archive for ZFN-mediated gene targeting. *Nat Methods* **9:** 588–590.

Guschin D, Waite A, Katibah G, Miller J, Holmes M, Rebar E. 2010. A rapid and general assay for monitoring endogenous gene modification. *Methods Mol Biol* **649:** 247–256.

Heinze S, Reppert SM. 2011. Sun compass integration of skylight cues in migratory monarch butterflies. *Neuron* **69:** 345–358.

The *Heliconius* Genome Consortium. 2012. Butterfly genome reveals promiscuous exchange of mimicry adaptations among species. *Nature* **487:** 94–98.

Ikeno T, Katagiri C, Numata H, Goto SG. 2011a. Causal involvement of mammalian-type cryptochrome in the circadian cuticle deposition rhythm in the bean bug *Riptortus pedestris*. *Insect Mol Biol* **20:** 409–415.
Ikeno T, Numata H, Goto SG. 2011b. Photoperiodic response requires mammalian-type cryptochrome in the bean bug *Riptortus pedestris*. *Biochem Biophys Res Commun* **410:** 394–397.
Kim HJ, Lee HJ, Kim H, Cho SW, Kim JS. 2009. Targeted genome editing in human cells with zinc finger nucleases constructed via modular assembly. *Genome Res* **19:** 1279–1288.
Kobayashi Y, Tanaka M, Ando H. 2003. Embryology. In *Lepidoptera, moths and butterflies: Morphology, physiology, and development* (ed. NP Kristensen), Chapter 19. De Gruyter, Berlin.
Lee C, Etchegaray JP, Cagampang FR, Loudon AS, Reppert SM. 2001. Posttranslational mechanisms regulate the mammalian circadian clock. *Cell* **107:** 855–867.
Marcus JM, Ramos DM, Monteiro A. 2004. Germline transformation of the butterfly *Bicyclus anynana*. *Proc Biol Sci* **271:** S263–S265.
Meng X, Noyes MB, Zhu LJ, Lawson ND, Wolfe SA. 2008. Targeted gene inactivation in zebrafish using engineered zinc-finger nucleases. *Nat Biotechnol* **26:** 695–701.
Merlin C, Gegear RJ, Reppert SM. 2009. Antennal circadian clocks coordinate sun compass orientation in migratory monarch butterflies. *Science* **325:** 1700–1704.
Miller JC, Holmes MC, Wang J, Guschin DY, Lee YL, Rupniewski I, Beausejour CM, Waite AJ, Wang NS, Kim KA, et al. 2007. An improved zinc-finger nuclease architecture for highly specific genome editing. *Nat Biotechnol* **25:** 778–785.
Mouritsen H, Frost BJ. 2002. Virtual migration in tethered flying monarch butterflies reveals their orientation mechanisms. *Proc Natl Acad Sci* **99:** 10162–10166.
Mussolino C, Cathomen T. 2012. TALE nucleases: Tailored genome engineering made easy. *Curr Opin Biotechnol* **23:** 644–650.
Peloquin JJ, Thibault ST, Staten R, Miller TA. 2000. Germ-line transformation of pink bollworm (Lepidoptera: gelechiidae) mediated by the *piggyBac* transposable element. *Insect Mol Biol* **9:** 323–333.
Perez SM, Taylor OR, Jander R. 1997. A Sun compass in monarch butterflies. *Nature* **387:** 29.
Porteus MH, Baltimore D. 2003. Chimeric nucleases stimulate gene targeting in human cells. *Science* **300:** 763.
Reppert SM. 2006. A colorful model of the circadian clock. *Cell* **124:** 233–236.
Reppert SM, Gegear RJ, Merlin C. 2010. Navigational mechanisms of migrating monarch butterflies. *Trends Neurosci* **33:** 399–406.
Robinson GE, Hackett KJ, Purcell-Miramontes M, Brown SJ, Evans JD, Goldsmith MR, Lawson D, Okamuro J, Robertson HM, Schneider DJ. 2011. Creating a buzz about insect genomes. *Science* **331:** 1386.
Szczepek M, Brondani V, Büchel J, Serrano L, Segal DJ, Cathomen T. 2007. Structure-based redesign of the dimerization interface reduces the toxicity of zinc-finger nucleases. *Nat Biotechnol* **25:** 786–793.
Takasu Y, Kobayashi I, Beumer K, Uchino K, Sezutsu H, Sajwan S, Carroll D, Tamura T, Zurovec M. 2010. Targeted mutagenesis in the silkworm *Bombyx mori* using zinc finger nuclease mRNA injection. *Insect Biochem Mol Biol* **40:** 759–765.
Tamura T, Thibert C, Royer C, Kanda T, Abraham E, Kamba M, Komoto N, Thomas JL, Mauchamp B, Chavancy G, et al. 2000. Germline transformation of the silkworm *Bombyx mori* L. using a *piggyBac* transposon-derived vector. *Nat Biotechnol* **18:** 81–84.
Terenius O, Papanicolaou A, Garbutt JS, Eleftherianos I, Huvenne H, Kanginakudru S, Albrechtsen M, An C, Aymeric JL, Barthel A, et al. 2011. RNA interference in Lepidoptera: An overview of successful and unsuccessful studies and implications for experimental design. *J Insect Physiol* **57:** 231–245.
Urnov FD, Rebar EJ, Holmes MC, Zhang HS, Gregory PD. 2010. Genome editing with engineered zinc finger nucleases. *Nat Rev Genet* **11:** 636–646.
Watanabe T, Ochiai H, Sakuma T, Horch HW, Hamaguchi N, Nakamura T, Bando T, Ohuchi H, Yamamoto T, Noji S, et al. 2012. Non-transgenic genome modifications in a hemimetabolous insect using zinc-finger and TAL effector nucleases. *Nat Comm* **3:** 1017.
Yuan Q, Metterville D, Briscoe AD, Reppert SM. 2007. Insect cryptochromes: Gene duplication and loss define diverse ways to construct insect circadian clocks. *Mol Biol Evol* **24:** 948–955.
Zhan S, Merlin C, Boore JL, Reppert SM. 2011. The monarch butterfly genome yields insights into long-distance migration. *Cell* **147:** 1171–1185.
Zhu H, Yuan Q, Briscoe AD, Froy O, Casselman A, Reppert SM. 2005. The two CRYs of the butterfly. *Curr Biol* **15:** R953–R954.
Zhu H, Sauman I, Yuan Q, Casselman A, Emery-Le M, Emery P, Reppert SM. 2008. Cryptochromes define a novel circadian clock mechanism in monarch butterflies that may underlie sun compass navigation. *PLoS Biol* **6:** e4. doi: 10.1371/journal.pbio.0060004.
Zhu C, Smith T, McNulty J, Rayla AL, Lakshmanan A, Siekmann AF, Buffardi M, Meng X, Shin J, Padmanabhan A, et al. 2011. Evaluation and application of modularly assembled zinc-finger nucleases in zebrafish. *Development* **138:** 4555–4564.

Received July 6, 2012; accepted in revised form September 21, 2012.